

# UC Irvine

## UC Irvine Previously Published Works

### Title

Stronger Contributions of Urbanization to Heat Wave Trends in Wet Climates

### Permalink

<https://escholarship.org/uc/item/4h03z2vh>

### Journal

Geophysical Research Letters, 45(20)

### ISSN

0094-8276

### Authors

Liao, Weilin

Liu, Xiaoping

Li, Dan

et al.

### Publication Date

2018-10-28

### DOI

10.1029/2018gl079679

### Copyright Information

This work is made available under the terms of a Creative Commons Attribution License, available at <https://creativecommons.org/licenses/by/4.0/>

Peer reviewed

## RESEARCH LETTER

10.1029/2018GL079679

## Key Points:

- HWs are becoming more frequent, longer-lasting, and stronger in most parts of China
- The contribution of urbanization to HW trends is larger and positive in wet climates but smaller and even negative in arid climates
- The stronger urbanization contribution to HW trends in wet climates is linked to the smaller variability of urban heat island intensity

## Supporting Information:

- Supporting Information S1

## Correspondence to:

X. Liu,  
liuxp3@mail.sysu.edu.cn

## Citation:

Liao, W., Liu, X., Li, D., Luo, M., Wang, D., Wang, S., et al. (2018). Stronger contributions of urbanization to heat wave trends in wet climates. *Geophysical Research Letters*, 45, 11,310–11,317. <https://doi.org/10.1029/2018GL079679>

Received 18 JUL 2018

Accepted 29 SEP 2018

Accepted article online 5 OCT 2018

Published online 16 OCT 2018

## Stronger Contributions of Urbanization to Heat Wave Trends in Wet Climates

Weilin Liao<sup>1,2</sup>, Xiaoping Liu<sup>1</sup>, Dan Li<sup>2</sup> , Ming Luo<sup>1,3</sup> , Dagang Wang<sup>1</sup>, Shaojian Wang<sup>1</sup>, Jane Baldwin<sup>4</sup> , Lijie Lin<sup>5</sup>, Xia Li<sup>6</sup>, Kuishuang Feng<sup>7</sup> , Klaus Hubacek<sup>7</sup>, and Xuchao Yang<sup>8</sup> 

<sup>1</sup>School of Geography and Planning, Sun Yat-sen University, Guangzhou, China, <sup>2</sup>Department of Earth and Environment, Boston University, Boston, MA, USA, <sup>3</sup>Institute of Environment, Energy and Sustainability, The Chinese University of Hong Kong, Hong Kong, <sup>4</sup>Program in Atmospheric and Oceanic Sciences, Princeton University, Princeton, NJ, USA, <sup>5</sup>School of Management, Guangdong University of Technology, Guangzhou, China, <sup>6</sup>Key Lab of Geographic Information Science (Ministry of Education), School of Geographic Sciences, East China Normal University, Shanghai, China, <sup>7</sup>Department of Geographical Sciences, University of Maryland, College Park, MD, USA, <sup>8</sup>Institute of Island and Coastal Ecosystems, Ocean College, Zhejiang University, Zhoushan, China

**Abstract** It is well known that urban areas are typically hotter than the surrounding (vegetated) rural areas. However, the contribution of urbanization to the trends of extreme temperature events such as heat waves (HWs) is less understood. Using a homogenized meteorological dataset drawn from nearly 2,000 stations in China, we find that urban and rural areas have different HW trends and the urban-rural contrast of HW trends varies across climate regimes. In wet climates, the increasing trends of HWs in urban areas are greater than those in rural areas, suggesting a positive contribution of urbanization to HW trends. In arid regions, the urbanization contribution to HW trends is smaller and even negative. The stronger urbanization contribution to HW trends in wet climates is linked to the smaller variability of urban heat island intensity. This study highlights the important role of local hydroclimate in modulating the urbanization contribution to extreme temperatures.

**Plain Language Summary** Extreme temperature events commonly known as heat waves (HWs) have profound impacts on human health. While it is well known that urban temperatures are usually higher than their rural counterparts (i.e., the urban heat island effect), whether and how the urbanization contribution to HW trends varies across different climate regimes over a large domain remains unclear. In this study, we explore the urban-rural contrast of HW characteristics over mainland China. Our analysis shows that while both urban and rural HWs are becoming more frequent, longer-lasting, and stronger in most parts of China, their trends are different. Interestingly, we find that the local hydroclimate modulates the variability of daily UHI intensity, thus affecting the contribution of urbanization to the frequency and magnitude of HWs. The stronger contrasts between urban and rural HW trends in wet climates are related to the larger increases in UHI intensity, but more importantly, the smaller variability of UHI intensity. As a result, the eastern, wet climate part of China, with the densest population and highest urbanization, will face severe heat risks in the future due to the combined effects of urbanization and global climate change.

### 1. Introduction

The frequency and magnitude of heat waves (HWs), which are a spell of consecutive hot days, have increased over recent decades, exerting a profound impact on human health (Easterling et al., 2000; Meehl & Tebaldi, 2004). Prolonged exposure to extremely hot days has been shown to not only increase the incidence of cardiovascular and respiratory diseases but also to increase mortality rates, especially for the elderly and the poor (Huang et al., 2011). The number of deaths caused by HWs has increased remarkably in recent years—from less than 6,000 in the period 1991–2000 to 136,000 in the past decade (2001–2010; WMO, 2013). In addition, HWs cause large-scale crop losses, forest fires, and increased energy consumption (Easterling et al., 2000; Peng et al., 2004).

In addition to the global effects of cumulative greenhouse gas emission, urbanization also plays an important role in inducing surface warming at local scales (Sun et al., 2016). The process of urban expansion is often characterized as a drastic transition in land use types accompanied by changes in land surface properties such as albedo, soil moisture, and heat storage. While it is well known that urban areas are typically hotter

than the surrounding (vegetated) rural areas (Yang et al., 2011; Zhou et al., 2004)—referred to as the *urban heat island effect*—the contribution of urbanization to extreme temperature event or HW trends remains understudied. A number of recent studies observed that urbanization has a significant impact on the trends of extreme temperature events over the eastern and southeastern parts of China (Luo & Lau, 2017; Ren & Zhou, 2014; Sun et al., 2014; Yang et al., 2017). However, whether and how the urbanization contribution to HW trends varies across different climate regimes over a large domain are still unclear (Papalexiou et al., 2018). More importantly, the key factors controlling the spatial variability of the urbanization contribution to HW trends have not been identified. Addressing these questions frames the scope of this study.

To do so, we use a homogenized surface air temperature data set collected from nearly 2,000 meteorological stations in mainland China over 54 summer seasons and identify HW events based on 12 different definitions commonly used in the literature (Smith et al., 2012). By exploring the urban-rural contrast of HW characteristics, our results show that local hydroclimate plays an important role in modulating the urbanization contribution to the HW trends. Specifically, the urbanization contribution to the HW trends is stronger in wet regions than in arid regions.

The paper is organized as follows: section 2 introduces the materials and methods used in this study. Section 3 presents and discusses the main results. Concluding remarks are made in section 4.

## 2. Materials and Methods

### 2.1. Materials

Meteorological data from 2,474 national stations in China are used in this study. These are collected from the China Meteorological Data Service Center (<http://data.cma.cn/>) for 54 summer seasons (i.e., May to September) from 1961 to 2014. The raw temperature data have been controlled for quality and homogenized using the method described by Xu et al. (2013). A station is treated as missing if it had five or more missing days in any summer season, and a total of 1,964 stations are retained for the analyses of the study.

Time varying land use/land cover maps of China are generated using Landsat TM/ETM+ images with a spatial resolution of 30 m (Liu et al., 2014). These maps are provided by the Data Center for Resources and Environmental Sciences, Chinese Academy of Sciences (<http://www.resdc.cn>) and are available for six episodes, that is, 1980, 1990, 1995, 2000, 2005, and 2010. Figure S1 shows the expansion of urban areas based on these maps. According to the time interval of the available maps, we divide the 1961–2014 period into six subperiods (1961–1980, 1981–1990, 1991–1995, 1996–2000, 2001–2005, and 2006–2014) for analysis. The builtup area is determined for each subperiod using the map at the end of the period, except in the last subperiod when the builtup area is determined using the 2010 map.

### 2.2. Definition of HW

HWs are commonly known as a spell of consecutive hot days. Many temperature metrics have been used to define a HW event, including daily maximum surface air temperature and daily mean surface air temperature (Anderson & Bell, 2011; Meehl & Tebaldi, 2004; Peng, Bobb, et al., 2011). However, consecutive hot days without limited nighttime relief have more significant increases of mortality and morbidity (Chen & Zhai, 2017; Hansen et al., 2008). Several recent studies have thus also defined HWs based on daily minimum surface air temperature in order to better capture the health effects of HWs (Chen & Zhai, 2017; Sillmann et al., 2013; Yang et al., 2017). Here we use 12 different HW definitions commonly used in the literature to define HWs as shown in the supporting information (Table S1 in the supporting information; Anderson & Bell, 2011; Chen & Zhai, 2017; Luo & Lau, 2017; Nath & Lau, 2014; Meehl & Tebaldi, 2004; Peng, Bobb, et al., 2011; Yang et al., 2017). It is not our goal to identify the *best* HW definition. Rather, we use these 12 definitions to explore whether our results are sensitive to the choice of HW definition. There are four HW indices defined based on daily mean temperature (HI01–HI04), four indices based on daily maximum temperature (HI05–HI08), and four indices based on daily minimum temperature (HI09–HI12). HI09–HI12 are created with the same definitions as HI05–HI08, except that daily maximum temperature is replaced by daily minimum temperature. The period of 1961–1990 is chosen as the base period to determine the thresholds in HW definitions. In this study, we focus on the following HW characteristics: the yearly number of HW events (HWN), the yearly sum of HW days (HWF), and the highest temperature of the hottest event (HWA).

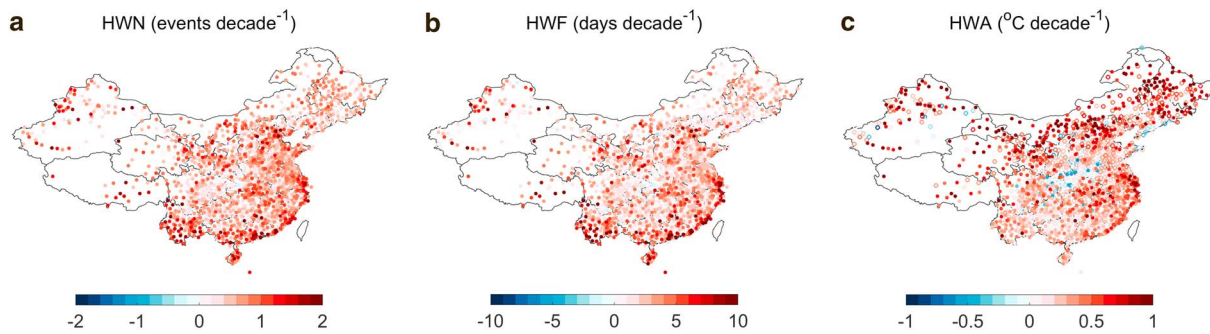


**Figure 1.** Linear trends of heat wave (HW) characteristics in 1961–2014. HW events are defined based on the twelfth HW index (HI12, see Table S1). (a) The yearly number of HW events (HWN). (b) The yearly sum of HW days (HWF). (c) The highest temperature of the hottest event (HWA). Solid circles denote stations with trends that are significant at the 95% confidence level, while open circles denote stations with insignificant trends.

### 2.3. Classification of Urban and Rural Stations

To explore the urbanization effect on surface warming, population data, satellite measurements of nighttime light data, or land use/land cover data are often used to classify stations into urban and rural types. However, most previous studies defined urban and rural stations based on a single time slice of classification data (i.e., a static scheme), despite the fact that those studies often included a long study period (Ren et al., 2015; Stone, 2007). China has experienced rapid urban development in recent decades, which caused numerous stations classified as rural in earlier periods to become urban in later periods. Previous studies found that the impact of urbanization on surface warming will be underestimated if the reference stations are selected based on a static scheme throughout the entire analysis period (Liao et al., 2017; Yang et al., 2011).

In this study, we dynamically classify stations based on time varying land use/land cover data. Following previous studies (Liao et al., 2017; Ren & Zhou, 2014; Yang et al., 2017), circular buffers with a radius of 2 km are established for each station and the proportion of builtup area within each circular buffer is then calculated. A larger proportion of builtup area means more urbanization around the station. Stations with 33% or more builtup area in the buffer zone are thus classified as urban stations, otherwise they are classified as rural stations (Ren & Zhou, 2014). In view of the rural-to-urban station conversions, the proportion of builtup area is updated for each station. The update frequency depends on the availability of land use/land cover data. Using the dynamic classification scheme, Figure S2 shows the spatial distribution of urban and rural stations in 1980, 1990, 1995, 2000, 2005, and 2010. In 1980, 332 stations (approximately 16.9% of total stations) were classified as urban. These stations were mainly located in northern China, central-eastern China, the coastal regions, and the capital of each province (Figure S2a). Many rural stations in these regions were converted to urban stations over the period 1980–2010. In particular, most of the stations in south China experienced rural-to-urban conversions. In 2010, the number of urban stations increased to 1022 (approximately 52.0% of total stations).

### 2.4. Estimation of the Urban-Rural Contrast of HW Characteristics

To estimate the urban-rural contrast of HW characteristics, we divide the study region into  $5^\circ \times 5^\circ$  latitude-longitude grids. Thirty-nine grid cells with at least one urban station, and one rural station are available throughout the entire period (see the shaded grid cells in Figure S2). The HW characteristics (i.e., HWN, HWF, and HWA) are calculated individually for each station, and then the HW characteristics of all the urban (rural) stations within the grid cell are averaged to construct the urban (rural) HW characteristics at the grid level. To exclude the topographical effect on grid-averaged HW characteristics, stations converted from rural to urban are discarded if their elevations are 500-m higher than the lowest height among the rural-to-urban stations within that grid cell.

## 3. Results and Discussion

### 3.1. Long-Term Changes of HWs in China

Figure 1 shows the long-term changes in the yearly number of HW events (HWN), the yearly sum of HW days (HWF), and the highest temperature of the hottest event (HWA), using 1 of the 12 HW definitions (HI12). It is

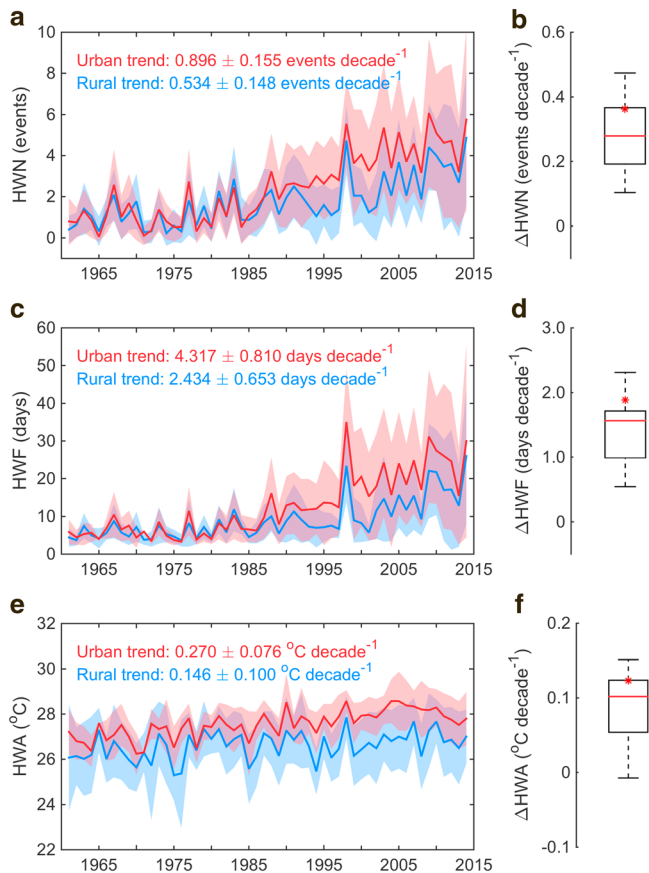


**Figure 2.** The differences between urban and rural heat waves (HWs) in 1961–2014. The left panels show the yearly statistics of urban (red) and rural (blue) a HWN, (c) HWF, and e HWA in the Pearl River Delta (20°N–25°N, 110°E–115°E) based on the twelfth HW index (HI12). The right panels are boxplots showing the urban-rural contrast in trends in (b) HWN, (d) HWF, and (f) HWA derived from the 12 different definitions, and the red asterisk denotes the results from HI12. Parameters in (a), (c), and (e) are the linear trends of urban and rural HWs, and the bounds indicate their corresponding 95% confidence intervals. The shading represents the mean  $\pm$  standard deviation among urban or rural stations within the grid cell.

clear that HWs become more frequent, longer-lasting, and stronger in most parts of China during the study period. The greatest increases of HWN appear in southern China and northwestern China, with a growth rate up to one to two events per decade, whereas the increases in HWF are up to 6–10 days per decade. In terms of the magnitude of HWs, the increasing trends of HWA in northern China are generally larger than those in southern China and exceed 0.5 °C per decade in the north. These results are consistent with those of previous studies (Chen & Zhai, 2017) and are robust across the 12 HW definitions (not shown).

### 3.2. The Urban-Rural Contrast of HW Trends

In this section, the urban and rural HW characteristics (HWN, HWF, and HWA) within each 5° × 5° grid cell are compared. Figure 2 shows the evolutions of urban and rural HW characteristics during 1961–2014 in the Pearl River Delta (20°N–25°N, 110°E–115°E), one of the grid cells that has experienced the most rapid urban growth in recent decades in the world (see Figure S1). It can be seen that the trends of urban HWs are stronger than those of rural HWs, across all 12 HW definitions. Taking the HI12 definition as an example, the urban-rural contrast of HWN, HWF, and HWA trends are 0.279  $\pm$  0.111 events/decade (mean  $\pm$  standard deviation), 1.564  $\pm$  0.534 days/decade, and 0.102  $\pm$  0.049 °C/decade in the Pearl River Delta, respectively. These urban-rural differences are stronger when HW is defined based on daily minimum surface air temperature, a finding that we relate to the stronger impact exerted by urbanization on nighttime surface air temperature than on its daytime counterpart (Liao et al., 2017; Ren & Zhou, 2014).

The same analysis is repeated for all 39 grid cells (5° × 5°) in mainland China. As expected, the urban-rural contrast of HW trends are not uniform (Figure S3). Overall, urbanization intensifies HW trends in most parts of eastern China but has a smaller and even negative impact in northwest China. The smaller and negative impact of urbanization on HW trends is consistent with the *urban cool islands* often found in desert climates that arise from irrigation and greening infrastructures in urban areas (Peng, Piao, et al., 2011; Zhou et al., 2014). These spatial patterns of urbanization contribution to HW trends are consistent

with previous research that studied the urbanization effect on trends of extreme temperature indices over mainland China (Chen & Zhai, 2017). However, previous research did not identify the key controlling factors of such spatial patterns, which motivates our analysis in the following section.

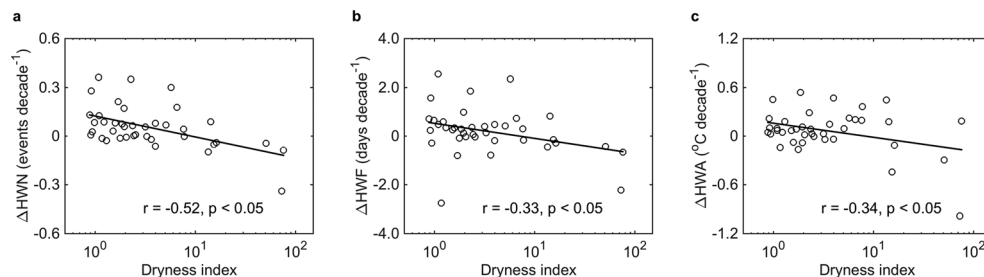


**Figure 3.** Relationship between urban-rural contrast of HW trends and the dryness index. Each point is the median of the urban-rural contrast of trends in (a) HWN, (b) HWF, and (c) HWA calculated from the 12 different HW definitions. The  $r$  denotes the correlation coefficient, all significant at 95% level.

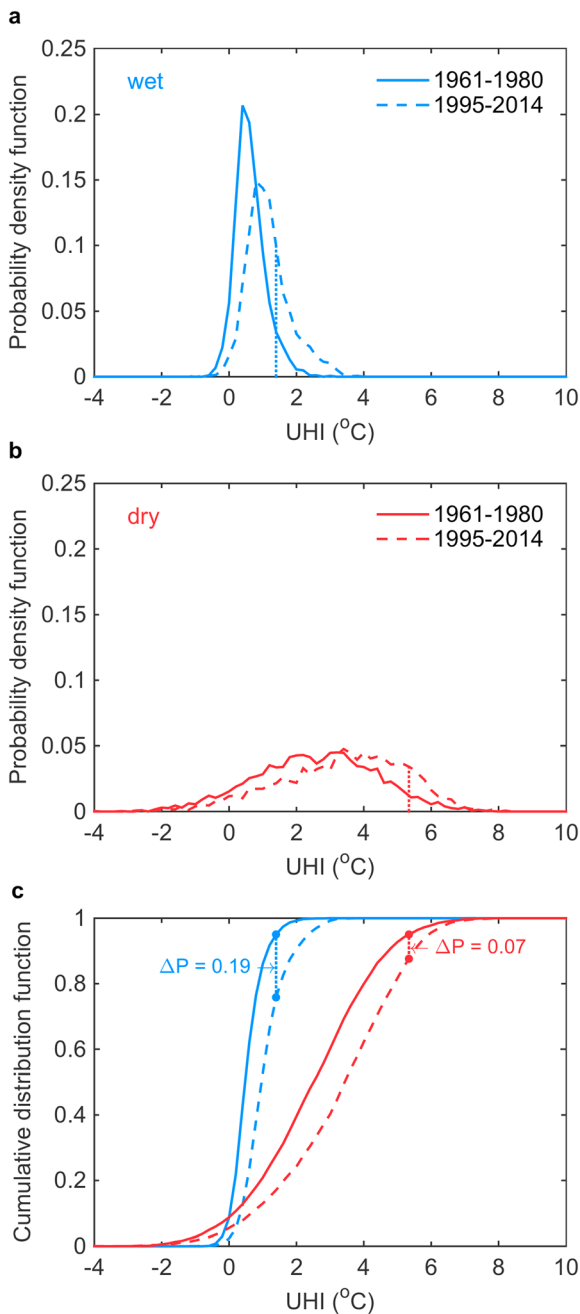


**Figure 4.** Probability and cumulative distribution functions of urban heat island (UHI) intensity. (a) Probability density function of UHI intensity in a wet grid cell during the periods 1961–1980 (historical period, solid curve) and 1995–2014 (current period, dashed curve), respectively. (b) Probability density function of UHI intensity in a dry grid cell during the periods 1961–1980 and 1995–2014, respectively. (c) The corresponding cumulative distribution functions of UHI intensity in the wet (blue) and dry (red) grid cells. The wet grid cell is located within the Pearl River Delta (20°N–25°N, 110°E–115°E), and the dry grid cell is situated within the Xinjiang region (40°N–45°N, 85°E–90°E). The vertical lines in (a) and (b) denote the probability of the 95th percentile value during the historical period.  $\Delta P$  in c denotes the changes in the probability of the 95th percentile value between the historical period and the current period. The UHI intensity is defined as the difference in daily minimum surface air temperature between urban and rural stations (i.e., urban minus rural).

### 3.3. Controlling Factors of the Spatial Variation of Urbanization Contribution to HW Trends

According to Figure S1, the urban growth rate is faster in eastern China but relatively slower in western China (Liu et al., 2017). We first hypothesize that the spatial variability of the urban-rural contrast of HW trends is controlled by the urban growth rate. To test this hypothesis, we examine the relationship between the urban-rural contrast of HW trends and the growth of builtup area, which we define as the increase in urban areas from 1980 to 2010 (Figure S4). Our results do not, however, reveal any significant correlation between them, suggesting that the spatial variation in the urbanization contribution to HW trends is not completely controlled by the spatial variation of urban growth rate.

On the other hand, the local hydroclimate is wetter in southeast China and drier in northwest China (Wang et al., 2017). Recent studies have shown that the annual mean urban heat island (UHI) intensity defined based on the land surface temperature increases with the annual mean precipitation, which is caused by the fact that precipitation controls the urban-rural contrast of surface roughness (Zhao et al., 2014) and evaporation (Gu & Li, 2017). Motivated by these studies, we further hypothesize that the spatial variability of the urban-rural contrast of HW trends can be explained by the local hydroclimate. To test this hypothesis, we explore the relation between the urban-rural contrast of HW trends and the dryness index, which is defined as the ratio of annual mean potential evaporation to annual mean precipitation over the study period and indicates the local hydroclimate (the higher the dryness index, the drier the region). Interestingly, the local hydroclimate is found to play a significant role in modulating the urban-rural contrast of HW trends (Figure 3). We also conduct a multivariate analysis using both the urban growth rate and the dryness index and calculate their partial correlation coefficients with urban-rural contrast of HW trends (Table S2). The partial correlation coefficients indicate that the urban growth rate is not significantly correlated with the urban-rural contrast of HW trends but the dryness index is. The role of dryness is more significant when HW is defined based on daily minimum temperature, followed by daily mean temperature and daily maximum temperature (Table S3). Hence, the rest of the analysis is mainly discussed based on daily minimum temperature.

Conceptually, the increasing occurrence of urban HWs in wet climates, relative to dry climates, can be induced by a shift of the UHI intensity probability density function (PDF) toward a larger mean and/or the change in its width (e.g., standard deviation or  $\sigma_{\text{UHI}}$ ; Schär et al., 2004). Note that here we are comparing the urban-rural HW contrasts in wet climates to those in dry climates (Figure 4), rather than comparing urban HWs to rural HWs. As a result, our reference is the results under dry climates (Figure 4b). We find that the PDF of UHI intensity in wet climates shifts toward a larger mean more rapidly than that in dry climates (cf. 1961–1980 and 1995–2014 in Figures 4a and 4b), as also evidenced by the fact that the trend of UHI intensity decreases with increasing dryness index (Figure S5). The relation, however, is insignificant and thus cannot fully explain the significant trends observed in Figure 3.

On the other hand, we find that compared to  $\sigma_{\text{UHI}}$  in dry climates,  $\sigma_{\text{UHI}}$  in wet climates is smaller especially when UHI is defined with daily minimum temperature measure (Figure S6a), which means that the PDF is wider and

flatter in dry climates (Figures 4a and 4b). The difference of  $\sigma_{\text{UHI}}$  between wet and dry climates is critically important because as the two PDFs (in wet and dry climates) shift toward larger mean values, the increase in the probability of extremely large (e.g., 95th percentile) values occurring is larger for the PDF with a smaller  $\sigma_{\text{UHI}}$ . The effect of this contrast can be further illustrated in the corresponding cumulative distribution functions: the probability for extremely large UHI intensity (e.g., 95th percentile) to occur increases more in wet climates because of the smaller  $\sigma_{\text{UHI}}$  (Figure 4c).

Now the question we need to address is why the UHI intensity shows a larger variability in dry climates. First, we find that the larger UHI variability in dry climates is related to the larger variability in both urban and rural temperatures (Figures S6b and S6c), implying that the larger UHI variability is related to processes that affect both urban and rural temperatures. Second, we find that daily UHI intensities on nonrainy days are significantly different from those on rainy days (Figure S7), suggesting that a larger variability of daily precipitation may lead to a larger variability of daily UHI intensity. In fact, the variability of daily precipitation increases with the dryness index ( $r = 0.67, p < 0.05$ ), which indicates that the variability of daily precipitation is larger in dry climates than in wet climates (Figure S8). As a result,  $\sigma_{\text{UHI}}$  is positively correlated with the variability of daily precipitation ( $r = 0.27, p < 0.1$ ; Figure S9). This positive correlation between  $\sigma_{\text{UHI}}$  and the variability of daily precipitation (Figure S9), together with the fact that the UHI intensities on nonrainy days are significantly different from their counterparts on rainy days (Figure S7), suggests that the larger variability of UHI intensity in dry climates is at least in part induced by the larger variability of precipitation. An additional factor contributing to the greater temperature variability in dry climates lies in the sensitivity of surface energy partitioning to precipitation variability. An arid, moisture limited regime can exhibit greater variance of temperature because changes in precipitation strongly affect the partitioning of latent/sensible heat fluxes. In contrast, in a wet regime where moisture is not limited, the partitioning of latent/sensible heat fluxes is less affected by changes in precipitation.

Lastly, to explore whether the relationship between the urban-rural contrast of HW trends and the dryness index is affected by the different station classification methods, we repeat our analysis using the static method (namely, classifying stations into urban and rural types only based on the land use/land cover data in 2010). The results show that the negative correlations between the urban-rural contrast of HW trends and the dryness index are robust even when urban and rural stations are classified using the static method (Figure S10). Hence, both static and dynamic station classification methods consistently show that local hydroclimate plays an important role in controlling the urban-rural contrast of HW trends. Moreover, to evaluate whether the relationship between  $\sigma_{\text{UHI}}$  and dryness is affected by the uneven distribution of meteorological stations (more stations in the east than in the west), we randomly select 20 stations from each grid cell and recalculate the correlation. This experiment is repeated 1,000 times. The resulting correlations are within the range of 0.27–0.54, and over 99% of them are significant at the 95% level. These results confirm a robust and significant relationship between  $\sigma_{\text{UHI}}$  and dryness, which is not caused by the difference in the number of stations.

In summary, our analysis shows that the local hydroclimate controls the urbanization contribution to HW trends through modulating the variability of daily UHI intensity. The stronger contrast between urban and rural HW trends in wet climates is related to the larger increasing trends of UHI intensity, but more importantly, the smaller variability of UHI intensity.

#### 4. Conclusions

In this study, we use a homogenized surface air temperature dataset collected from nearly 2,000 meteorological stations in mainland China to identify HW events based on 12 commonly used definitions. Additionally, we dynamically classify stations based on time varying land use/land cover data and examine the long-term changes in the urban-rural contrast of HW characteristics (i.e., HWN, HWF, and HWA). The results show that HWs are becoming more frequent, longer-lasting, and stronger in both urban and rural areas across most parts of China. However, the contribution of urbanization to the HW trends is greater in wet regions compared to in arid regions.

By exploring the control of the spatial variation of the urban-rural HW contrast, we show that the local hydroclimate modulates the variability of daily UHI intensity, thus affecting the contribution of urbanization to the

HW trends. The stronger contrast between urban and rural HW trends in wet climates is related to the larger increasing trends of UHI intensity, but more importantly, the smaller variability of UHI intensity. As a result, the eastern, wetter part of China, with the densest population and highest urbanization, will face increasingly severe heat risks in the future due to the combined effects of urbanization and global climate change (Li & Bou-Zeid, 2013). Our study strongly encourages the development and implementation of mitigation and adaptation strategies in order to combat the adverse effect of HWs, particularly in urban areas located in wet climates.

#### Acknowledgments

This study was supported by the National Natural Science Foundation of China (grants 41401052, 41671398, 41871029, 51379224, and 51579105), the Fundamental Research Funds for the Central Universities (grant 15lgjc), the Key National Science Foundation of China (grant 41531176), and the International Program for PhD candidates Sun Yat-sen University. The authors are thankful to the China Meteorological Data Service Center and the Data Center for Resources and Environmental Sciences of the Chinese Academy of Sciences for providing the meteorological data (<http://data.cma.cn/>) and land use/land cover maps (<http://www.resdc.cn>), respectively.

#### References

- Anderson, G. B., & Bell, M. L. (2011). Heat waves in the United States: Mortality risk during heat waves and effect modification by heat wave characteristics in 43 U.S. communities. *Environmental Health Perspectives*, *119*(2), 210–218. <https://doi.org/10.1289/ehp.1002313>
- Chen, Y., & Zhai, P. (2017). Revisiting summertime hot extremes in China during 1961–2015: Overlooked compound extremes and significant changes. *Geophysical Research Letters*, *44*, 5096–5103. <https://doi.org/10.1002/2016GL072281>
- Easterling, D. R., Meehl, G. A., Parmesan, C., Changnon, S. A., Karl, T. R., & Mearns, L. O. (2000). Climate extremes: Observations, modeling, and impacts. *Science*, *289*(5487), 2068–2074. <https://doi.org/10.1126/science.289.5487.2068>
- Gu, Y., & Li, D. (2017). A modeling study of the sensitivity of urban heat islands to precipitation at climate scales. *Urban Climate*, *24*, 982–993. <https://doi.org/10.1016/j.uclim.2017.12.001>
- Hansen, A., Bi, P., Nitschke, M., Ryan, P., Pisaniello, D., & Tucker, G. (2008). The effect of heat waves on mental health in a temperate Australian City. *Environmental Health Perspectives*, *116*(10), 1369–1375. <https://doi.org/10.1289/ehp.11339>
- Huang, C., Barnett, A. G., Wang, X., Vaneckova, P., FitzGerald, G., & Tong, S. (2011). Projecting future heat-related mortality under climate change scenarios: A systematic review. *Environmental Health Perspectives*, *119*(12), 1681–1690. <https://doi.org/10.1289/ehp.1103456>
- Li, D., & Bou-Zeid, E. (2013). Synergistic interactions between urban Heat Islands and heat waves: The impact in cities is larger than the sum of its parts. *Journal of Applied Meteorology and Climatology*, *52*(9), 2051–2064. <https://doi.org/10.1175/JAMC-D-13-02.1>
- Liao, W., Wang, D., Liu, X., Wang, G., & Zhang, J. (2017). Estimated influence of urbanization on surface warming in eastern China using time-varying land use data. *International Journal of Climatology*, *37*(7), 3197–3208. <https://doi.org/10.1002/joc.4908>
- Liu, J., Kuang, W., Zhang, Z., Xu, X., Qin, Y., Ning, J., et al. (2014). Spatiotemporal characteristics, patterns, and causes of land-use changes in China since the late 1980s. *Journal of Geographical Sciences*, *24*(2), 195–210. <https://doi.org/10.1007/s11442-014-1082-6>
- Liu, X., Liang, X., Li, X., Xu, X., Ou, J., Chen, Y., et al. (2017). A future land use simulation model (FLUS) for simulating multiple land use scenarios by coupling human and natural effects. *Landscape and Urban Planning*, *168*, 94–116. <https://doi.org/10.1016/j.landurbplan.2017.09.019>
- Luo, M., & Lau, N.-C. (2017). Heat waves in southern China: Synoptic behavior, long-term change, and urbanization effects. *Journal of Climate*, *30*(2), 703–720. <https://doi.org/10.1175/JCLI-D-16-0269.1>
- Meehl, G. A., & Tebaldi, C. (2004). More intense, more frequent, and longer lasting heat waves in the 21st century. *Science*, *305*(5686), 994–997. <https://doi.org/10.1126/science.1098704>
- Nath, M. J., & Lau, N.-C. (2014). Model simulation and projection of European heat waves in present-day and future climates. *Journal of Climate*, *27*(10), 3713–3730. <https://doi.org/10.1175/JCLI-D-13-00284.1>
- Papalexiou, S. M., AghaKouchak, A., Trenberth, K. E., & Foufoula-Georgiou, E. (2018). Global, regional, and megacity trends in the highest temperature of the year: Diagnostics and evidence for accelerating trends. *Earth's Future*, *6*, 71–79. <https://doi.org/10.1002/2017EF000709>
- Peng, R. D., Bobb, J. F., Tebaldi, C., McDaniel, L., Bell, M. L., & Dominici, F. (2011). Toward a quantitative estimate of future heat wave mortality under global climate change. *Environmental Health Perspectives*, *119*(5), 701–706. <https://doi.org/10.1289/ehp.1002430>
- Peng, S., Huang, J., Sheehy, J. E., Laza, R. C., Visperas, R. M., Zhong, X., et al. (2004). Rice yields decline with higher night temperature from global warming. *Proceedings of the National Academy of Sciences of the United States of America*, *101*(27), 9971–9975. <https://doi.org/10.1073/pnas.0403720101>
- Peng, S., Piao, S., Ciais, P., Friedlingstein, P., Ottle, C., Bréon, F.-M., et al. (2011). Surface urban Heat Island across 419 global big cities. *Environmental Science & Technology*, *46*(2), 696–703. <https://doi.org/10.1021/es2030438>
- Ren, G., & Zhou, Y. (2014). Urbanization effect on trends of extreme temperature indices of national stations over mainland China, 1961–2008. *Journal of Climate*, *27*(6), 2340–2360. <https://doi.org/10.1175/JCLI-D-13-00393.1>
- Ren, Y., Li, J., Chu, Z., Zhang, A., Zhou, Y., Zhang, L., et al. (2015). An integrated procedure to determine a reference station network for evaluating and adjusting urban bias in surface air temperature data. *Journal of Applied Meteorology and Climatology*, *54*(6), 1248–1266. <https://doi.org/10.1175/JAMC-D-14-0295.1>
- Schär, C., Vidale, P. L., Lüthi, D., Frei, C., Häberli, C., Liniger, M. A., & Appenzeller, C. (2004). The role of increasing temperature variability in European summer heatwaves. *Nature*, *427*(6972), 332–336. <https://doi.org/10.1038/nature02300>
- Sillmann, J., Kharin, V. V., Zwiers, F. W., Zhang, X., & Bronaugh, D. (2013). Climate extremes indices in the CMIP5 multimodel ensemble: Part 2. Future climate projections. *Journal of Geophysical Research: Atmospheres*, *118*, 2473–2493. <https://doi.org/10.1002/jgrd.50188>
- Smith, T. T., Zaitchik, B. F., & Gohlke, J. M. (2012). Heat waves in the United States: Definitions, patterns and trends. *Climatic Change*, *118*(3–4), 811–825. <https://doi.org/10.1007/s10584-012-0659-2>
- Stone, B. (2007). Urban and rural temperature trends in proximity to large US cities: 1951–2000. *International Journal of Climatology*, *27*(13), 1801–1807. <https://doi.org/10.1002/joc.1555>
- Sun, Y., Zhang, X., Ren, G., Zwiers, F. W., & Hu, T. (2016). Contribution of urbanization to warming in China. *Nature Climate Change*, *6*(7), 706–709. <https://doi.org/10.1038/nclimate2956>
- Sun, Y., Zhang, X., Zwiers, F. W., Song, L., Wan, H., Hu, T., et al. (2014). Rapid increase in the risk of extreme summer heat in eastern China. *Nature Climate Change*, *4*(12), 1082–1085. <https://doi.org/10.1038/nclimate2410>
- Wang, Z., Xie, P., Lai, C., Chen, X., Wu, X., Zeng, Z., & Li, J. (2017). Spatiotemporal variability of reference evapotranspiration and contributing climatic factors in China during 1961–2013. *Journal of Hydrology*, *544*, 97–108. <https://doi.org/10.1016/j.jhydrol.2016.11.021>
- WMO (2013). *The global climate 2001–2010: A decade of climate extremes*. Switzerland: World Meteorological Organization.
- Xu, W., Li, Q., Wang, X. L., Yang, S., Cao, L., & Feng, Y. (2013). Homogenization of Chinese daily surface air temperatures and analysis of trends in the extreme temperature indices. *Journal of Geophysical Research: Atmospheres*, *118*, 9708–9720. <https://doi.org/10.1002/jgrd.50791>

- Yang, X., Hou, Y., & Chen, B. (2011). Observed surface warming induced by urbanization in east China. *Journal of Geophysical Research*, *116*, D14113. <https://doi.org/10.1029/2010JD015452>
- Yang, X., Leung, L. R., Zhao, N., Zhao, C., Qian, Y., Hu, K., et al. (2017). Contribution of urbanization to the increase of extreme heat events in an urban agglomeration in east China. *Geophysical Research Letters*, *44*, 6940–6950. <https://doi.org/10.1002/2017GL074084>
- Zhao, L., Lee, X., Smith, R. B., & Oleson, K. (2014). Strong contributions of local background climate to urban heat islands. *Nature*, *511*(7508), 216–219. <https://doi.org/10.1038/nature13462>
- Zhou, D., Zhao, S., Liu, S., Zhang, L., & Zhu, C. (2014). Surface urban heat island in China's 32 major cities: Spatial patterns and drivers. *Remote Sensing of Environment*, *152*, 51–61. <https://doi.org/10.1016/j.rse.2014.05.017>
- Zhou, L., Dickinson, R. E., Tian, Y., Fang, J., Li, Q., Kaufmann, R. K., et al. (2004). Evidence for a significant urbanization effect on climate in China. *Proceedings of the National Academy of Sciences of the United States of America*, *101*(26), 9540–9544. <https://doi.org/10.1073/pnas.0400357101>